Supplement: Parameterising secondary organic aerosol formation from α-pinene using a detailed oxidation and aerosol formation model

Karl Ceulemans, Steven Compernolle, Jean-François Müller

July 26, 2011

1 Generic Chemistry: Description

1.1 Generic species

The generic chemistry system was introduced in Capouet et al. (2008), and further extended in Ceulemans et al. (2010). Generic species are defined by their carbon number (from 10 down to 6) and by one explicit functional group. The generic species are further subdivided into 11 volatility classes. Each class represents lumped organic compounds, which have a 'parent compound' (the molecule resulting from replacement of the explicit functional group by one or more hydrogen atoms) with a saturated liquid vapour pressure $p^0_{\mathrm{L,parent}}$ falling within the volatility class range. For the highest volatility class, indicated by the letter 'a', $p^0_{\mathrm{L,parent}} > 10^{-1}$ Torr at 298 K. Class 'b' contains species with 10^{-1} Torr $> p^0_{\mathrm{L,parent}} > 10^{-1.5}$ Torr, etc., and for class 'k', $p^0_{\mathrm{L,parent}} < 10^{-5.5}$ Torr.

In our notation a generic species name consists of the prefix 'LX', the carbon number, the vapour pressure class symbol and the explicit functional group. In total there are 55 classes (5 carbon numbers times eleven vapour pressure classes), besides the generic products with less than 6 carbon atoms, which are not considered for SOA formation, and lumped into a special generic class (with prefix 'SX').

The vapour pressure of a (non-radical) generic species is determined by the contribution of its explicit group (see Table 1), and the representative volatility class vapour pressure $p^0_{\mathrm{L,LX}}$, which at 298 K is equal to the geometric mean of the volatility class range for classes 'b'-'j', $10^{-0.75}$ Torr for class 'a', and $10^{-5.75}$ Torr for class 'k'. The temperature dependence of $p^0_{\mathrm{L,LX}}$ is estimated based on Makar (2001).

Table 1: Overview of generic species.

Generic species	Explicitly represented group	$\Delta \log_{10} p^0_{\mathrm{group}}$ (Capouet and Müller, 2006)	Note
LX10eOOH	hydroperoxide	$-2.9942 + 0.0332(T - 298)$	
LX10eOH	alcohol	$-2.0374 + 0.0124(T - 298)$	
LX10eCHO	aldehyde	$-0.8937 + 0.0124(T - 298)$	a
LX10eCAR	keto-aldehyde	$-1.787 + 0.0248(T - 298)$	a
LX10eKET	ketone	$-0.8937 + 0.0124(T - 298)$	
LX10ePAN	peroxy acyl nitrate	$-2.5372 + 0.0113(T - 298)$	a,b
LX10eONO2	nitrate	$-1.6711 + 0.0063(T - 298)$	
LX10eCOOH	carboxylic acid	$-3.2516 + 0.0075(T - 298)$	a
LX10eCOOOH	peroxy acid	$-3.2516 + 0.0075(T - 298)$	a
LX10eO	alkoxy radical		
LX10eO2	peroxy radical		
LX10e03	acyl peroxy radical		

[a] The carbons in this explicit group are already accounted for in the implicit part of the species.
[b] The contribution of the PAN group in Capouet and Müller (2006) has been reduced in the current version of BOREAM. Uncertainty is very high, however, as vapour pressures for only one compound have been experimentally determined.

1.2 Generic reactions

In the following tables, the reactions for one category of generic species are listed. The reaction rates and products are based on the reaction rates and product distributions for similar explicit compounds.

1.2.1 Reactions of molecular generic species

Table 2: Reactions of generic molecular species: illustration for LX10e. R2R and RO3 are peroxy radical counters (see Capouet et al., 2004).

Reactants	Products	Reaction rate	Note
LX10eOOH + OH	→ LX10eCHO + OH	k_{seth}	a
LX10eOOH + OH	→ LX10kO2 + R2R	0.4 k_{LX}	g
	→ LX10iO3 + RO3	0.3 k_{LX}	h
	→ LX10eCHO + OH	0.3 k_{LX}	i
LX10eOH + OH	→ LX10eCHO + HO_2	k_{seth}	b
LX10eOH + OH	→ LX10iO2 + R2R	0.4 k_{LX}	g
	→ LX10gO3 + RO3	0.3 k_{LX}	h
	→ LX10cCHO + OH	0.3 k_{LX}	i
LX10eCHO + OH	→ LX10eO3 + RO3	k_{carb}	c
LX10eCHO + NO_3	→ LX10eO3 + RO3 + HNO_3	k_{NO_3}	d
LX10eCHO + OH	→ LX10gO2 + R2R	0.4 k_{LX}	g
	→ LX10eO3 + RO3	0.3 k_{LX}	h
	→ LX10aCHO + OH	0.3 k_{LX}	i
LX10eCAR + OH	→ LX10gO3 + RO3	k_{carb}	c
LX10eCAR + NO_3	→ LX10gO3 + RO3 + HNO_3	k_{NO_3}	d
LX10eCAR + OH	→ LX10iO2 + R2R	0.4 k_{LX}	g
	→ LX10gO3 + RO3	0.3 k_{LX}	h
	→ LX10cCHO + OH	0.3 k_{LX}	i
LX10eKET + OH	→ LX10gO2 + R2R	0.4 k_{LX}	g
	→ LX10eO3 + RO3	0.3 k_{LX}	h
	→ LX10aCHO + OH	0.3 k_{LX}	i
LX10ePAN + OH	→ LX10kO2 + R2R + NO_2	0.4 k_{LX}	g
	→ LX10iO3 + RO3 + NO_2	0.3 k_{LX}	h
	→ LX10eCHO + OH + NO_2	0.3 k_{LX}	i
LX10eONO2 + OH	→ LX10eCHO + NO_2	0.07 k_{seth}	e
LX10eONO2 + OH	→ LX10hO2 + R2R + NO_2	0.4 k_{LX}	g
	→ LX10fO3 + RO3 + NO_2	0.3 k_{LX}	h
	→ LX10bCHO + OH + NO_2	0.3 k_{LX}	i
LX10eCOOH + OH	→ LX9dO2 + R2R + CO_2	$k_{\text{H-abst.ROH}}$	f,j
LX10eCOOH + OH	→ LX10kO2 + R2R	0.4 k_{LX}	g
	→ LX10iO3 + RO3	0.3 k_{LX}	h
	→ LX10eCHO + OH	0.3 k_{LX}	i
LX10eCOOOH + OH	→ LX10eO3 + H_2O + RO3	$k_{\text{H-abst.ROOH}}$	f,j
LX10eCOOOH + OH	→ LX10kO2 + R2R	0.4 k_{LX}	g
	→ LX10iO3 + RO3	0.3 k_{LX}	h
	→ LX10eCHO + OH	0.3 k_{LX}	i

[a],[b] $k_{\text{seth}} = 5.32 \times 10^{-12}\text{cm}^3\text{molecule}^{-1}\text{s}^{-1}$, based on the rate recommended by Neeb (2000) for abstraction of a secondary H from the α-carbon, bearing an -OH or -OOH group. H-abstraction from oxygen atoms is ignored.
[c] H-abstraction from the -CHO group: $k_{\text{carb}} = 16.9 \times 10^{-12}\text{cm}^3\text{molecule}^{-1}\text{s}^{-1}$, based on measurements reported by Atkinson et al. (2006) and Schurath and Naumann (2003).
[d] $k_{\text{NO}_3} = 1.67\ \exp(-1460/T)10^{-12}\text{cm}^3\text{molecule}^{-1}\text{s}^{-1}$ (Atkinson et al., 2006).
[e] based on Neeb (2000).
[f] based on Neeb (2000), for abstraction of an H attached to a single oxygen ($k_{\text{H-abst.ROH}} = 0.8 \times 10^{-12}\text{cm}^3\text{molecule}^{-1}\text{s}^{-1}$) or to a peroxy group ($k_{\text{H-abst.ROOH}} = 2.0 \times 10^{-12}\text{cm}^3\text{molecule}^{-1}\text{s}^{-1}$).
[g] H-abstraction from an implicit aliphatic carbon, leading to a peroxy radical.
[h] H-abstraction from an implicit aldehydic carbon, leading to an acyl peroxy radical.
[i] H-abstraction from an implicit carbon bearing an α-hydroperoxide function, leading to a carbonyl and an OH radical.
[g] to [i] : For OH-reactions with the implicit part og the generic compound; $k_{\text{LX}} = 8.0 \times 10^{-12}\text{cm}^3\text{molecule}^{-1}\text{s}^{-1}$. The branching ratios of the reaction pathways described in notes [g] to [i] depend on the presence of functional groups in the parent structure, and therefore also on its vapour pressure (as vapour pressure and functionalisation are correlated). We assume these branching ratios have the values (0.6,0.2,0.2) for classes 'a' to 'c', (0.4,0.3,0.3) for classes 'd'-'g' and (0.2,0.4,0.4) for classes 'h'-'k'.

1.2.2 Photolysis of molecular generic species

Table 3: Photolysis of molecular generic species: illustration for LX10e.

Reactants	Products	Reaction rate	Note
LX10eOOH + hν	→ LX10eO + OH	2 · j(LXCH3OOH)	a,b
LX10eOOH + hν	→ LX8aOOH + CH3CHO	j(LXALD)	c
LX10eOH + hν	→ LX10cO + OH	j(LXCH3OOH)	b
LX10eOH + hν	→ LX8aOH + CH3CHO	j(LXALD)	c
LX10eCHO + hν	→ LX8cO2 + R2R + CH3CHO	0.8 · j(ALD)	a,d
	→ LX9dO2 + R2R + CO	0.2 · j(ALD)	
LX10eCHO + hν	→ LX10aO + OH	j(LXCH3OOH)	b
LX10eCHO + hν	→ LX8aCHO + CH3CHO	j(LXALD)	c
LX10eCAR + hν	→ LX8eKET + CH3CHO	0.8 · j(ALD)	a
	→ LX9fO2 + R2R + CO	0.2 · j(ALD)	
LX10eCAR + hν	→ LX7dKET + CH3CHO	0.8 · j(keto)	
	→ LX8eO2 + R2R + CH3CO	0.2 · j(keto)	
LX10eCAR + hν	→ LX10cO + OH	j(LXCH3OOH)	b
LX10eCAR + hν	→ LX8aCOOOH + CH3CHO	j(LXALD)	c
LX10eKET + hν	→ LX8cO2 + R2R + CH3CHO	0.8 · j(keto)	a,d
LX10eKET + hν	→ LX8cO2 + R2R + CH3CO3 + RO3	0.2 · j(keto)	
LX10eKET + hν	→ LX10aO + OH	j(LXCH3OOH)	b
LX10eKET + hν	→ LX8aKET + CH3CHO	j(LXALD)	c
LX10ePAN + hν	→ LX10eO3 + NO2 + RO3	0.8 · j(ppn)	a
LX10ePAN + hν	→ LX10eO2 + NO3 + R2R	0.2 · j(ppn)	
LX10ePAN	→ LX10eO3 + NO2 + RO3	k_{PAN}	a
LX10ePAN + hν	→ LX10eO + OH + NO2	j(LXCH3OOH)	b
LX10ePAN + hν	→ LX8aPAN + CH3CHO	j(LXALD)	c
LX10eONO2 + hν	→ LX10eO + NO2	j(nitu)	a
LX10eONO2 + hν	→ LX10aO + OH + NO2	j(LXCH3OOH)	b
LX10eONO2 + hν	→ LX8bONO2 + CH3CHO	j(LXALD)	c
LX10eCOOH + hν	→ LX10eO + OH	j(LXCH3OOH)	b
LX10eCOOH + hν	→ LX8aCOOH + CH3CHO	j(LXALD)	c
LX10eCOOOH + hν	→ LX9dO2 + R2R + CO2 + OH	j(peracid)	a
LX10eCOOOH + hν	→ LX10eO + OH	j(LXCH3OOH)	b
LX10eCOOOH + hν	→ LX8aCOOOH + CH3CHO	j(LXALD)	c

[a] The J-values for photolysis of the explicitly represented groups and the product distributions follow Capouet et al. (2004) and Capouet et al. (2008).

[b],[c] Photolysis of the implicit part of the molecule, assumed to proceed as for a compound containing one hydroperoxide group (b) and one aldehyde group (c). For classes 'a' to 'd', the J-values are halved, due to expected lower functionalisation.

[b] Photolysis of a hydroperoxide group in the implicit part of the compound, resulting in an alkoxy radical and OH.

[c] Aldehyde photolysis in the implicit part is assumed to follow the Norrish-type II reaction, which leads to an alkene and ethaldehyde (see Paulson et al., 2006). This results in removal of 2 carbons and the aldehyde group from the implicit part of the generic species, increasing volatility (here from class 'e' to 'a').

[d] For explicit aldehyde and ketone photolysis, branching ratios of 0.8 for Norrish-type II reaction (leading to an alkene and ethaldehyde), and 0.2 for the radical channel are assumed. In the first case, the alkene is then assumed to quickly react with OH or ozone, yielding a peroxy radical.

1.2.3 Generic alkoxy radical reactions

Table 4: Reactions of generic alkoxy radicals: illustration with the radical LX10eO.

Reactants	Products	Branching ratios	Note
LX10eO + O_2	→ LX10eCHO + HO_2	0.15	a,g
LX10eO	→ LX9dO2 + R2R + CH_2O	0.3	b,f,g
	→ LX9bO3 + RO3 + CH_2O	0.1	f
	→ LX9aCHO + OH + CH_2O	0.1	f
LX10eO	→ LX9aO2 + R2R + HCOOH	0.05	c,g
LX10eO	→ LX7aO2 + R2R + acetone	0.10	d,g
LX10eO	→ LX10iO2 + R2R	0.12	e,f,g
	→ LX10gO3 + RO3	0.04	f
	→ LX10cCHO + OH	0.04	f

[a] Assumed branching ratio for reaction with O_2.
[b] We consider three types of decomposition, with the most common being of the type RCH2O· → R· + CH_2O.
[c] This decomposition follows RCH(OH)O· → R· + HCOOH .
[d] This decomposition reaction follows R(CH3CO·CH3) → R· + acetone .
[e] H-shift isomerisation, as in RCH2CH2CH2CH2O· → RC·HCH2CH2CH2OH .
[f] An alkyl radical is produced. Alkyl radicals without an α-functionality react with O_2, forming peroxy radicals. However, alkyl radicals bearing an α-aldehyde function generate acyl alkoxy radicals, and in case of a possible α-hydroperoxide, the radical becomes an aldehyde + OH. The assumed branching ratios for these three possible pathways are $(0.6, 0.2, 0.2)$ for classes 'e' to 'k' and $(0.8, 0.1, 0.1)$ for classes 'a' to 'd'.
[g] The branching ratios depend on the vapour pressure class (see Table 5).

Table 5: Branching ratios for generic alkoxy radicals depending on their vapour pressure class.

Alkoxy radical reaction pathway	class a-c	class d-g	class h-k
reaction with O_2	0.20	0.15	0.05
CH_2O elimination	0.40	0.5	0.65
HCOOH elimination	0.05	0.05	0.05
acetone elimination	0.05	0.10	0.15
H-shift isomerisation	0.30	0.2	0.10

Decomposition is more likely for the more chemically functionalised species (see for example Vereecken and Peeters, 2009). Therefore, the assumed branching ratios for decomposition increase with decreasing vapour pressure, since we assume an inverse correlation between number of functional groups present and vapour pressure.

1.2.4 Generic peroxy radical reactions

Table 6: Reactions of generic peroxy radicals: illustration with radical LX10eO2.

Reactants	Products	Reaction rate	Note
LX10eO2 + NO	→ LX10eO + NO2 - R2R	$0.9 \cdot k_{\mathrm{NO,RO_2}}$	a,b
LX10eO2 + NO	→ LX10eONO2 - R2R	$0.1 \cdot k_{\mathrm{NO,RO_2}}$	a,b
LX10eO2 + NO3	→ LX10eO + NO2 - R2R	$k_{\mathrm{NO_3,RO_2}}$	a,c
LX10eO2 + HO2	→ LX10eOOH - R2R	$k_{\mathrm{HO_2,RO_2}}$	a,d
LX10eO2 + R3R	→ 0.70 LX10eO + 0.30 LX10eCHO	$k_{\mathrm{R2R,R3R}}$	a
LX10eO2 + R3O	→ 0.70 LX10eO + 0.30 LX10eCHO	$k_{\mathrm{R2R,R3O}}$	a
LX10eO2 + R3H	→ 0.70 LX10eO + 0.30 LX10eCHO	$k_{\mathrm{R2R,R3H}}$	a
LX10eO2 + R2R	→ 0.50 LX10eO + 0.25 LX10eCHO + 0.25 LX10eOH	$k_{\mathrm{R2R,R2R}}$	a
LX10eO2 + R2O	→ 0.50 LX10eO + 0.25 LX10eCHO + 0.25 LX10eOH	$k_{\mathrm{R2R,R3R}}$	a
LX10eO2 + R2H	→ 0.50 LX10eO + 0.25 LX10eCHO + 0.25 LX10eOH	$k_{\mathrm{R2R,R2H}}$	a
LX10eO2 + R1R	→ 0.50 LX10eO + 0.25 LX10eCHO + 0.25 LX10eOH	$k_{\mathrm{R2R,R1R}}$	a
LX10eO2 + R1H	→ 0.50 LX10eO + 0.25 LX10eCHO + 0.25 LX10eOH	$k_{\mathrm{R2R,R1H}}$	a
LX10eO2 + RO3	→ LX10eO	$r_{\mathrm{oxyr}} \cdot k_{\mathrm{RO_2,RO_3}}$	a,e,f
LX10eO2 + RO3	→ LX10eCHO	$r_{\mathrm{acid}} \cdot k_{\mathrm{RO_2,RO_3}}$	a,e,f

[a] Peroxy radicals are grouped into 9 classes according to their functionality, and their cross reactions are then treated using a system of peroxy radical class counters (Capouet et al., 2004). Generic peroxy radicals are assumed to behave as the so-called R2R-class, which contains secondary peroxy radicals without α- or β-functional groups. The cross-reaction rates $k_{\mathrm{R2R,R3R}}$, etc., can be calculated using Table 2 and Eq. 3 in Capouet et al. (2004), and the product distributions follow Table 1 in Capouet et al. (2004).

[b] $k_{\mathrm{NO,RO_2}} = 2.54 \times 10^{-12} \exp(360/T)$ cm^3 molecule^{-1}s^{-1} (Saunders et al., 2003). The estimated alkyl nitrate yield is 0.1 (see Capouet et al. (2004))).

[c] $k_{\mathrm{NO_3,RO_2}} = 2.3 \times 10^{-12}$ cm^3 molecule^{-1}s^{-1}(based on $C_2H_5O_2$ in Atkinson et al. (2006)).

[d] $k_{\mathrm{HO_2,RO_2}} = 2.72 \times 10^{-13} \exp(1250/T)$ cm^3 molecule^{-1}s^{-1} (Saunders et al., 2003).

[e] For the cross-reactions between peroxy radicals and acyl peroxy radicals the rate constant $k_{\mathrm{RO_2,RO_3}} = 1.0{\times}10^{-11}$ cm^3 molecule^{-1}s^{-1} is used (Capouet et al., 2004).

[f] The branching ratios of the alkoxy radical channel and the molecular channel are given by $r_{\mathrm{acid}} = 1/(1 + 2.2 \cdot 10^6 \exp(-3280/T))$ and $r_{\mathrm{oxyr}} = 1 - r_{\mathrm{acid}}$.

1.2.5 Generic acyl peroxy radical reactions

Table 7: Reactions of generic acyl peroxy radicals: illustration with radical LX10eO3.

Reactants	Products	Reaction rate	Note
LX10eO3 + NO	→ CO_2 + 0.60 LX9dO2 + 0.60 R2R + 0.20 LX9bO3 + 0.20 RO3 + 0.20 LX9aCHO + 0.20 OH + NO2 - RO3	k_{NO,RO_3}	a,g
LX10eO3 + NO2	→ LX10ePAN - RO3	k_{NO_2,RO_3}	b
LX10eO3 + NO3	→ CO_2 + 0.60 LX9dO2 + 0.60 R2R + 0.20 LX9bO3 + 0.20 RO3 + 0.20 LX9aCHO + 0.20 OH + NO2 - RO3	k_{NO_3,RO_3}	c,g
LX10eO3 + HO2	→ LX10eCOOH + O3 - RO3	$0.13 \cdot k_{HO_2,RO_3}$	d
LX10eO3 + HO2	→ LX10eCOOOH + O2 - RO3	$0.41 \cdot k_{HO_2,RO_3}$	d
LX10eO3 + HO2	→ CO_2 + 0.60 LX9dO2 + 0.60 R2R + 0.20 LX9bO3 + 0.20 RO3 + 0.20 LX9aCHO + 0.20 OH + OH - RO3	$0.46 \cdot k_{HO_2,RO_3}$	d,g
LX10eO3 + R3R	→ CO_2 + 0.60 LX9dO2 + 0.60 R2R + 0.20 LX9bO3 + 0.20 RO3 + 0.20 LX9aCHO + 0.20 OH	k_{RO_2,RO_3}	e,g
LX10eO3 + R3O	→ CO_2 + 0.60 LX9dO2 + 0.60 R2R + 0.20 LX9bO3 + 0.20 RO3 + 0.20 LX9aCHO + 0.20 OH	k_{RO_2,RO_3}	g
LX10eO3 + R3H	→ CO_2 + 0.60 LX9dO2 + 0.60 R2R + 0.20 LX9bO3 + 0.20 RO3 + 0.20 LX9aCHO + 0.20 OH	k_{RO_2,RO_3}	g
LX10eO3 + R2R	→ CO_2 + 0.60 LX9dO2 + 0.60 R2R + 0.20 LX9bO3 + 0.20 RO3 + 0.20 LX9aCHO + 0.20 OH	$r_{oxyr} \cdot k_{RO_2,RO_3}$	g
LX10eO3 + R2R	→ LX10eCOOH	$r_{acid} \cdot k_{RO_2,RO_3}$	
LX10eO3 + R2O	→ CO_2 + 0.60 LX9dO2 + 0.60 R2R + 0.20 LX9bO3 + 0.20 RO3 + 0.20 LX9aCHO + 0.20 OH	$r_{oxyr} \cdot k_{RO_2,RO_3}$	g
LX10eO3 + R2O	→ LX10eCOOH	$r_{acid} \cdot k_{RO_2,RO_3}$	
LX10eO3 + R2H	→ CO_2 + 0.60 LX9dO2 + 0.60 R2R + 0.20 LX9bO3 + 0.20 RO3 + 0.20 LX9aCHO + 0.20 OH	$r_{oxyr} \cdot k_{RO_2,RO_3}$	g
LX10eO3 + R2H	→ LX10eCOOH	$r_{acid} \cdot k_{RO_2,RO_3}$	
LX10eO3 + R1R	→ CO_2 + 0.60 LX9dO2 + 0.60 R2R + 0.20 LX9bO3 + 0.20 RO3 + 0.20 LX9aCHO + 0.20 OH	$r_{oxyr} \cdot k_{RO_2,RO_3}$	g
LX10eO3 + R1R	→ LX10eCOOH	$r_{acid} \cdot k_{RO_2,RO_3}$	
LX10eO3 + R1O	→ CO_2 + 0.60 LX9dO2 + 0.60 R2R + 0.20 LX9bO3 + 0.20 RO3 + 0.20 LX9aCHO + 0.20 OH	$r_{oxyr} \cdot k_{RO_2,RO_3}$	g
LX10eO3 + R1O	→ LX10eCOOH	$r_{acid} \cdot k_{RO_2,RO_3}$	
LX10eO3 + R1H	→ CO_2 + 0.60 LX9dO2 + 0.60 R2R + 0.20 LX9bO3 + 0.20 RO3 + 0.20 LX9aCHO + 0.20 OH	$r_{oxyr} \cdot k_{RO_2,RO_3}$	g
LX10eO3 + R1H	→ LX10eCOOH	$r_{acid} \cdot k_{RO_2,RO_3}$	
LX10eO3 + RO3	→ CO_2 + 0.60 LX9dO2 + 0.60 R2R + 0.20 LX9bO3 + 0.20 RO3 + 0.20 LX9aCHO + 0.20 OH	k_{self,RO_3}	f

[a] $k_{NO,RO_3} = 6.7 \times 10^{-12} \exp(340/T)$ cm^3 molecule^{-1}s^{-1}, based on $C_2H_5CO(O_2)$ (Atkinson et al., 2006).
[b] k_{NO_2,RO_3} is calculated using the high-pressure limit of the Troe-expression for the $CH_3C(O)O_2 + NO_2$ reaction (see Capouet et al. (2004) and references therein), which in this case is $1.2 \cdot 10^{-11}(T/300)^{-0.9}$ cm^3 molecule^{-1}s^{-1} (Atkinson et al., 2006).
[c] $k_{NO_3,RO_3} = 4.3 \times 10^{-12}$ cm^3 molecule^{-1}s^{-1} based on $CH_3CO(O_2)$(Saunders et al., 2003).
[d] The product distribution is based on $CH_3C(O)O_2 + HO_2$ Jenkin et al. (2007). The reaction rate $k_{HO_2,RO_3} = 5.2 \times 10^{-13} \exp(983/T)$ cm^3 molecule^{-1}s^{-1} is used (see Capouet et al. (2004)).
[e] For the cross-reactions between peroxy radicals and acyl peroxy radicals the rate constant $k_{RO_2,RO_3} = 1.0 \times 10^{-11}$ cm^3 molecule^{-1}s^{-1} is used (Capouet et al., 2004).
[f] For the self-reactions of acyl peroxy radicals, $k_{self,RO_3} = 1.5 \times 10^{-11}$ cm^3 molecule^{-1}s^{-1} is used (Capouet et al., 2004).
[g] In these reactions an acyl alkoxy radical is produced, which decomposes into an alkyl radical and CO_2. Treatment of alkyl radicals follows note f in Table 4.

2 BOREAM Model validation

We present a comparison of measured time series for α-pinene, ozone, NO_x and SOA with simulations performed with the full BOREAM model. First we show simulations for a low-NO_x experiment (1) and a high-NO_x experiment (4) from Ng et al. (2007). The time series and discussion of some aspects concerning the simulations are given in Valorso et al. (2011). Initial concentrations for important species for which measurements were not available were optimised in order to obtain good agreement for observed α-pinene decay. For three experiments from Carter (2000) we compare the quantity $D(O_3 - NO) = ([O_3] - [O_3]_{\text{initial}}) - ([NO] - [NO]_{\text{initial}})$, which is an indication for the strength of ozone production.

Table 8: Initial settings for concentrations of VOC and inorganic compounds in the experiments 1 and 4 from Ng et al. (2007), discussed in Valorso et al. (2011). Optimised initial values and wall sources differ slightly from those in Valorso et al. (2011)

Initial settings	Exp. 1	Exp. 4
available measurements		
temperature	298 K	299 K
Relative humidity	5.3%	3.3%
[α-pinene]	13.8 ppb	12.6 ppb
[O_3]	4 ppb	not available
[NO]	not available	475 ppb
[NO_2]	not available	463 ppb
model settings for unmeasured parameters		
[O_3]	measured value	0 ppb
[NO]	0.35 ppb	measured value
[NO_2]	0.35 ppb	measured value
[H_2O_2]	1250 ppb	0 ppb
[HONO]	0 ppb	1000 ppb
$J(NO_2)$	$3.3 \cdot 10^{-1}\text{min}^{-1}$	$4.2 \cdot 10^{-1}\text{min}^{-1}$
$J(H_2O_2)$	$1.35 \cdot 10^{-4}\text{min}^{-1}$	$1.7 \cdot 10^{-4}\text{min}^{-1}$
NO wall source	0.5 ppt min^{-1}	none
NO_2 wall source	0.5 ppt min^{-1}	none
unknown OH source	none	$1.8 \cdot 10^{9}\text{molec cm}^3\text{s}^{-1}$
aerosol wall loss	$1.\cdot 10^{-5}$ s^{-1}	$1. \cdot 10^{-5}\text{s}^{-1}$

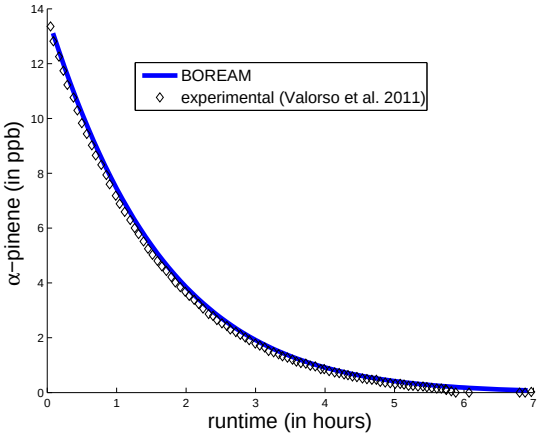

Figure 1: Measured and full BOREAM model α-pinene concentrations for experiment 1 of Ng et al. (2007).

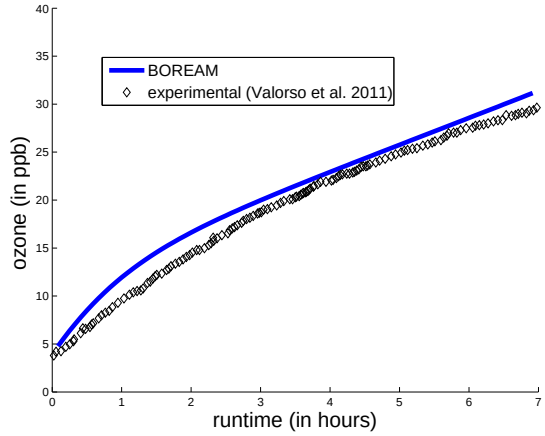

Figure 2: Measured and full BOREAM model ozone concentrations for experiment 1 of Ng et al. (2007).

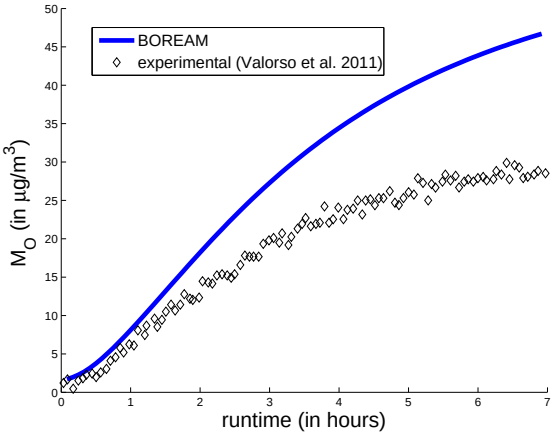

Figure 3: Measured and full BOREAM model SOA mass concentrations for experiment 1 of Ng et al. (2007).

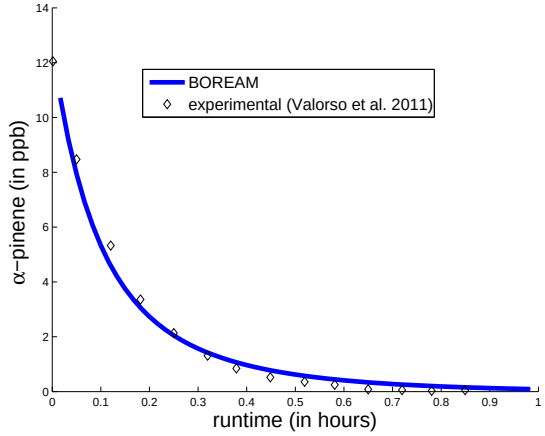

Figure 4: Measured and full BOREAM model α-pinene concentrations for experiment 4 of Ng et al. (2007).

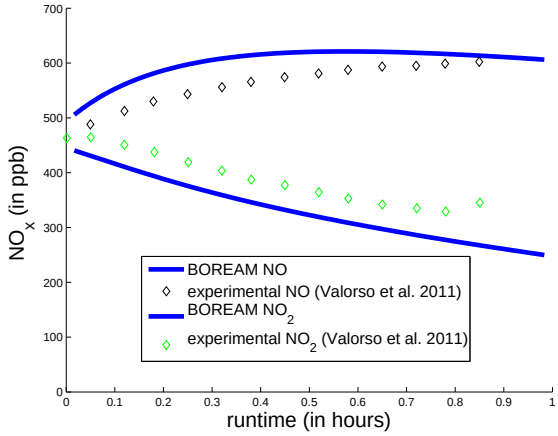

Figure 5: Measured and full BOREAM model NO and NO_2 concentrations for experiment 4 of Ng et al. (2007).

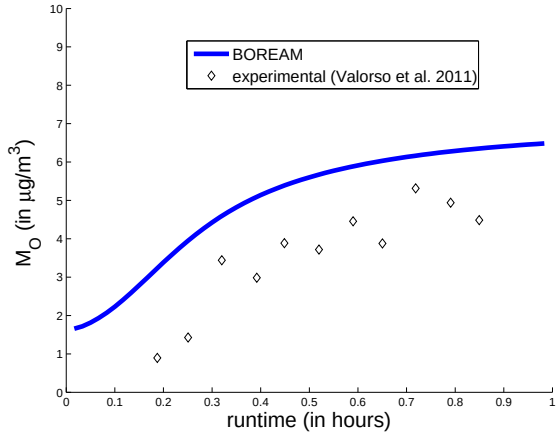

Figure 6: Measured and full BOREAM model SOA mass concentrations for experiment 4 of Ng et al. (2007).

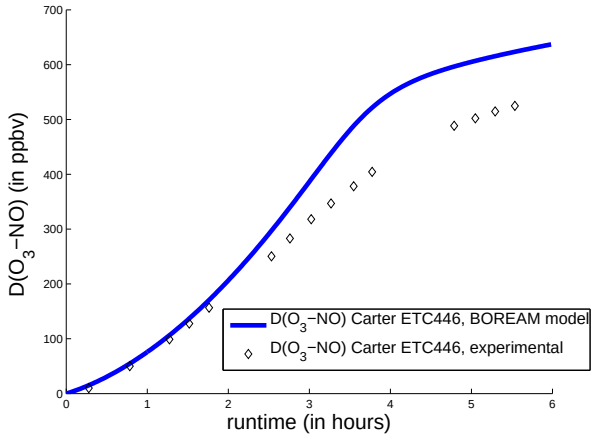

Figure 7: Measured and full BOREAM model $D(\mathrm{O_3} - \mathrm{NO})$ (in ppb) for experiment ETC446 of Carter (2000).

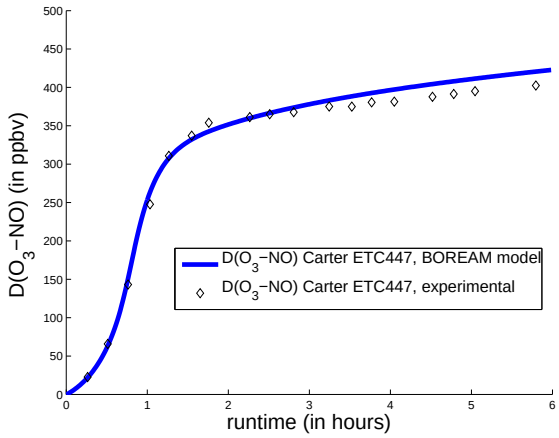

Figure 8: Measured and full BOREAM model $D(\mathrm{O_3 - NO})$ (in ppb) for experiment ETC447 of Carter (2000).

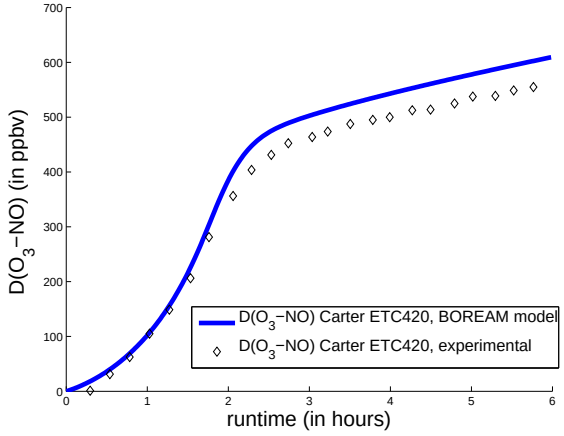

Figure 9: Measured and full BOREAM model $D(\mathrm{O_3 - NO})$ (in ppb) for experiment ETC420 of Carter (2000).

3 SOA parameterisation agreement with full model

The following Figs. 10 to 13 compare the SOA yield of the full and 10-product model, as a complement to Fig. 2 in the main part of the article. As a further validation of the parameter model at intermediate NO_x, Fig. 14 compares the full and parameterised yields at various NO_x-levels for the ozonolysis scenario. Figs. 15 to 18 show the agreement between full and parameter model for SOA formed under OH-oxidation at intermediate-NO_x and at temperatures between 273 K and 303 K.

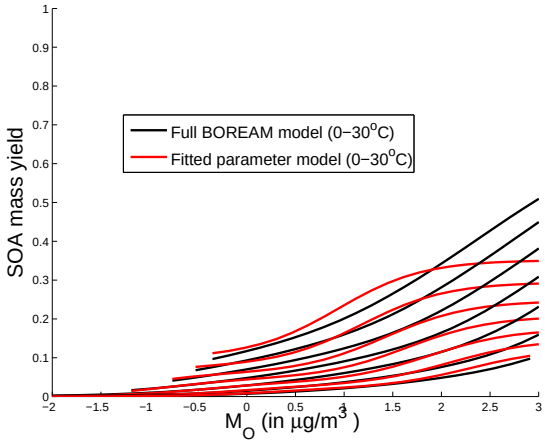

Figure 10: Parameterised and full model SOA mass yields in function of the logarithm of the organic aerosol mass loading M_O, for the high-NO_x OH-oxidation scenario. The seven curves are obtained at temperatures ranging from 0 to 30°C, by steps of 5°C, the last temperature corresponding to the lowest curve.

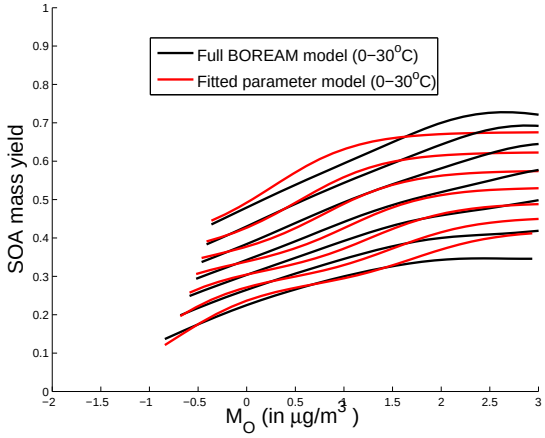

Figure 11: Idem as Fig. 10, but for the low-NO_x O_3-oxidation scenario.

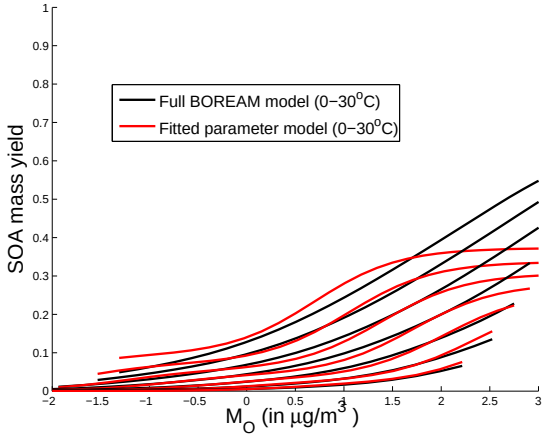

Figure 12: Idem as Fig. 10, but for the high-NO_x O_3-oxidation scenario.

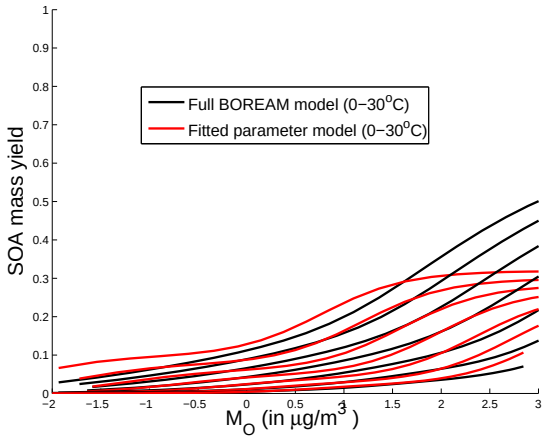

Figure 13: Idem as Fig. 10, but for the high-NO_x NO_3-oxidation scenario.

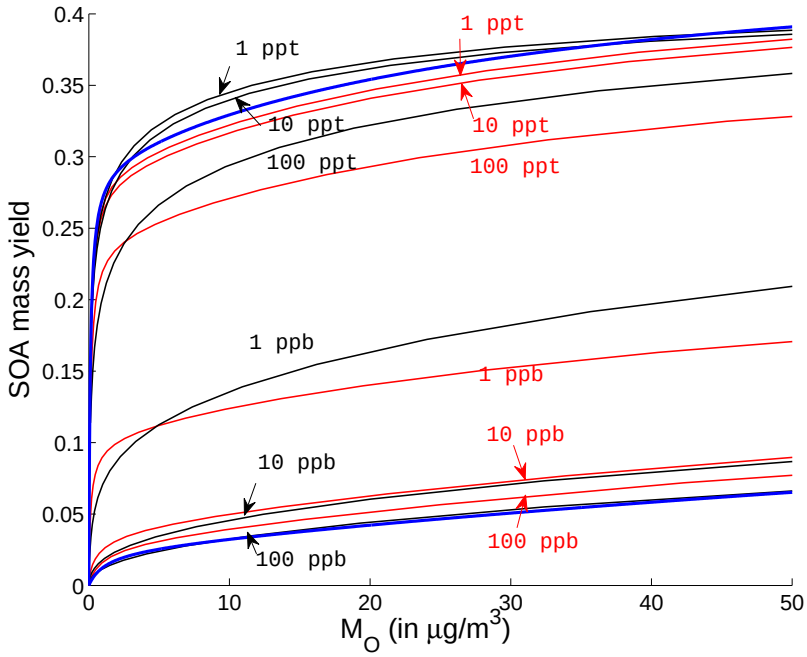

Figure 14: SOA yields calculated by the full (black) and parameterised (red) model at various NO_2 levels, for ozone oxidation (at 298 K). The parameterised functions $Y(M_O)$ for high and low NO_x concentrations are shown in blue.

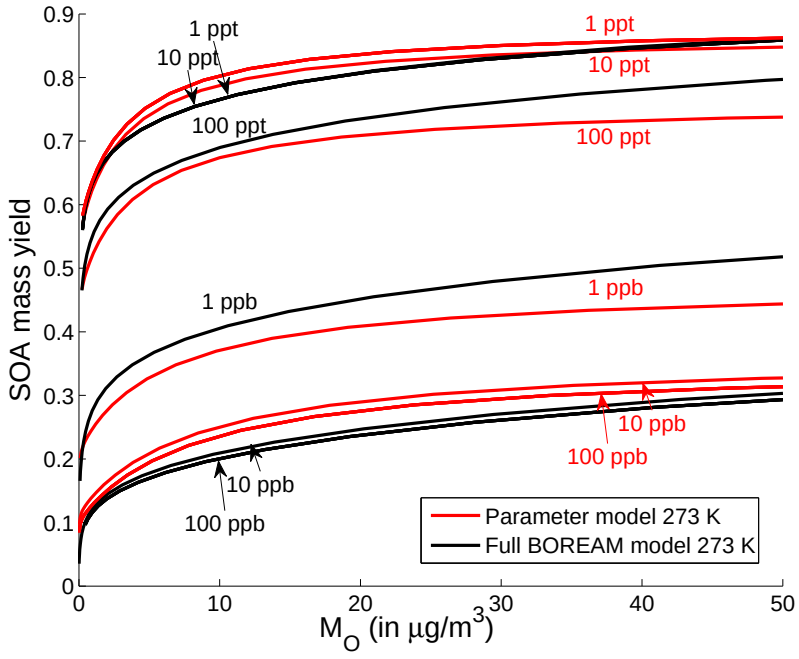

Figure 15: Comparison of full model (black) and parameter model (red) SOA mass yields in function of M_O for OH-oxidation, at 7 different NO_2 concentrations (at 273 K).

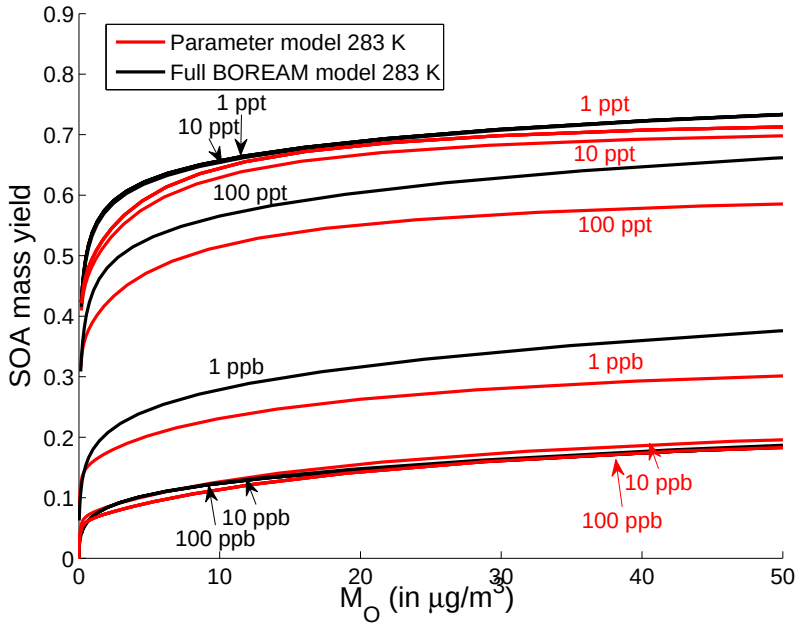

Figure 16: Comparison of full model (black) and parameter model (red) SOA mass yields in function of M_O for OH-oxidation, at 7 different NO_2 concentrations (at 283 K).

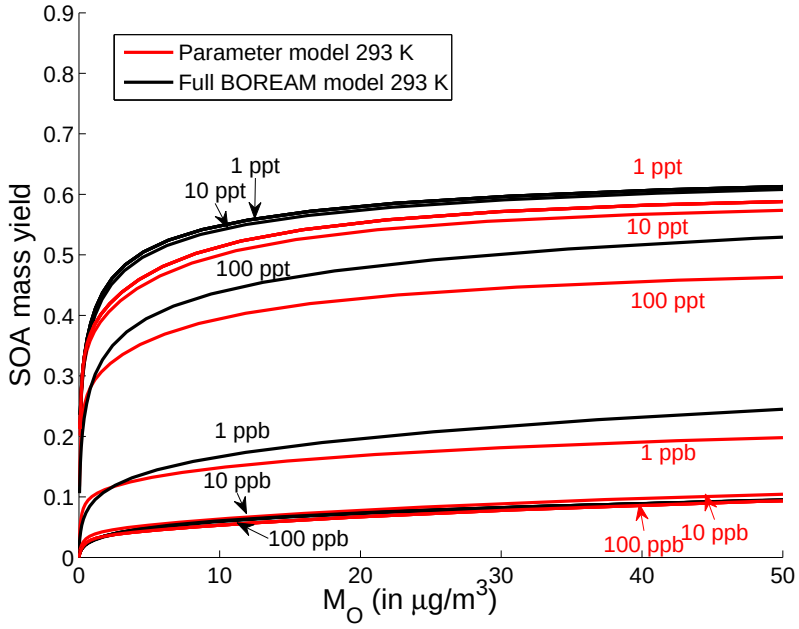

Figure 17: Comparison of full model (black) and parameter model (red) SOA mass yields in function of M_O for OH-oxidation, at 7 different NO_2 concentrations (at 293 K).

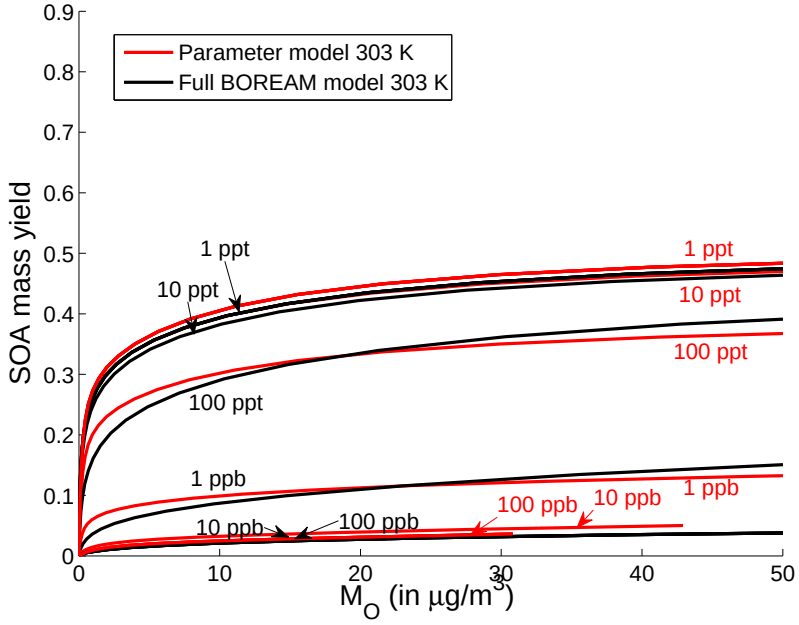

Figure 18: Comparison of full model (black) and parameter model (red) SOA mass yields in function of M_O for OH-oxidation, at 7 different NO_2 concentrations (at 303 K).

4 Parameterised activity coefficients for the 10-product model

γ_{H_2O} (activity coefficient of water) and γ_{Org} (pseudo-activity coefficient of the organic SOA fraction) are given at 100 RH-values from 0.5% up to 99.5%, at low NO_x (Table 9) and high NO_x (Table 10) for the OH-oxidation of α-pinene.

Table 9: Parameterised activity coefficients γ_{H_2O} and γ_{Org} for low-NO_x OH-oxidation.

RH (in %)	γ_{H_2O} (low-NO_x)	γ_{Org} (low-NO_x)	RH (in %)	γ_{H_2O} (low-NO_x)	γ_{Org} (low-NO_x)
0.5	0.4179	1.0018	50.5	0.8743	0.6885
1.5	0.4298	0.9998	51.5	0.8815	0.6807
2.5	0.4415	0.9977	52.5	0.8886	0.6728
3.5	0.4531	0.9955	53.5	0.8956	0.6650
4.5	0.4644	0.9930	54.5	0.9026	0.6572
5.5	0.4756	0.9902	55.5	0.9095	0.6495
6.5	0.4866	0.9872	56.5	0.9163	0.6418
7.5	0.4975	0.9838	57.5	0.9231	0.6341
8.5	0.5082	0.9800	58.5	0.9298	0.6265
9.5	0.5188	0.9760	59.5	0.9364	0.6189
10.5	0.5292	0.9716	60.5	0.9430	0.6113
11.5	0.5395	0.9669	61.5	0.9494	0.6038
12.5	0.5497	0.9619	62.5	0.9558	0.5964
13.5	0.5598	0.9566	63.5	0.9621	0.5890
14.5	0.5698	0.9510	64.5	0.9683	0.5816
15.5	0.5796	0.9452	65.5	0.9745	0.5743
16.5	0.5894	0.9392	66.5	0.9805	0.5671
17.5	0.5991	0.9330	67.5	0.9865	0.5599
18.5	0.6086	0.9266	68.5	0.9924	0.5527
19.5	0.6181	0.9201	69.5	0.9981	0.5456
20.5	0.6275	0.9135	70.5	1.0038	0.5385
21.5	0.6368	0.9067	71.5	1.0094	0.5315
22.5	0.6460	0.8998	72.5	1.0149	0.5245
23.5	0.6551	0.8928	73.5	1.0202	0.5176
24.5	0.6642	0.8858	74.5	1.0255	0.5107
25.5	0.6731	0.8787	75.5	1.0306	0.5038
26.5	0.6820	0.8715	76.5	1.0356	0.4970
27.5	0.6908	0.8643	77.5	1.0405	0.4903
28.5	0.6996	0.8570	78.5	1.0452	0.4837
29.5	0.7083	0.8497	79.5	1.0498	0.4771
30.5	0.7168	0.8423	80.5	1.0542	0.4707
31.5	0.7254	0.8349	81.5	1.0584	0.4644
32.5	0.7338	0.8275	82.5	1.0624	0.4583
33.5	0.7422	0.8200	83.5	1.0663	0.4524
34.5	0.7505	0.8125	84.5	1.0699	0.4467
35.5	0.7587	0.8050	85.5	1.0732	0.4414
36.5	0.7669	0.7974	86.5	1.0763	0.4364
37.5	0.7750	0.7898	87.5	1.0791	0.4319
38.5	0.7830	0.7822	88.5	1.0815	0.4279
39.5	0.7910	0.7745	89.5	1.0836	0.4245
40.5	0.7989	0.7668	90.5	1.0849	0.4215
41.5	0.8067	0.7590	91.5	1.0861	0.4194
42.5	0.8145	0.7512	92.5	1.0863	0.4187
43.5	0.8222	0.7435	93.5	1.0854	0.4204
44.5	0.8298	0.7356	94.5	1.0836	0.4255
45.5	0.8374	0.7278	95.5	1.0801	0.4360
46.5	0.8449	0.7199	96.5	1.0731	0.4589
47.5	0.8523	0.7121	97.5	1.0604	0.5181
48.5	0.8597	0.7042	98.5	1.0215	1.0164
49.5	0.8670	0.6964	99.5	1.0006	2.8443

Table 10: Parameterised activity coefficients γ_{H_2O} and γ_{Org} for high-NO_x OH-oxidation.

RH (in %)	γ_{H_2O} (high-NO_x)	γ_{Org} (high-NO_x)	RH (in %)	γ_{H_2O} (high-NO_x)	γ_{Org} (high-NO_x)
0.5	0.5486	0.9983	50.5	0.9409	0.8416
1.5	0.5580	0.9930	51.5	0.9474	0.8415
2.5	0.5672	0.9875	52.5	0.9538	0.8415
3.5	0.5764	0.9819	53.5	0.9602	0.8416
4.5	0.5855	0.9763	54.5	0.9665	0.8418
5.5	0.5945	0.9706	55.5	0.9727	0.8422
6.5	0.6034	0.9650	56.5	0.9789	0.8427
7.5	0.6123	0.9594	57.5	0.9850	0.8433
8.5	0.6211	0.9539	58.5	0.9910	0.8440
9.5	0.6299	0.9485	59.5	0.9970	0.8448
10.5	0.6386	0.9432	60.5	1.0029	0.8458
11.5	0.6472	0.9381	61.5	1.0087	0.8469
12.5	0.6557	0.9331	62.5	1.0144	0.8481
13.5	0.6642	0.9282	63.5	1.0201	0.8495
14.5	0.6727	0.9235	64.5	1.0257	0.8509
15.5	0.6811	0.9189	65.5	1.0312	0.8525
16.5	0.6894	0.9145	66.5	1.0367	0.8543
17.5	0.6977	0.9103	67.5	1.0420	0.8561
18.5	0.7059	0.9062	68.5	1.0473	0.8582
19.5	0.7140	0.9022	69.5	1.0525	0.8603
20.5	0.7221	0.8985	70.5	1.0576	0.8627
21.5	0.7302	0.8948	71.5	1.0626	0.8652
22.5	0.7382	0.8913	72.5	1.0675	0.8678
23.5	0.7461	0.8880	73.5	1.0723	0.8707
24.5	0.7540	0.8847	74.5	1.0769	0.8738
25.5	0.7618	0.8816	75.5	1.0815	0.8772
26.5	0.7696	0.8787	76.5	1.0860	0.8808
27.5	0.7774	0.8758	77.5	1.0903	0.8847
28.5	0.7850	0.8731	78.5	1.0944	0.8889
29.5	0.7927	0.8705	79.5	1.0985	0.8935
30.5	0.8002	0.8680	80.5	1.1023	0.8986
31.5	0.8078	0.8657	81.5	1.1060	0.9041
32.5	0.8152	0.8634	82.5	1.1095	0.9101
33.5	0.8227	0.8612	83.5	1.1128	0.9168
34.5	0.8300	0.8592	84.5	1.1159	0.9242
35.5	0.8374	0.8573	85.5	1.1188	0.9324
36.5	0.8446	0.8555	86.5	1.1214	0.9415
37.5	0.8518	0.8538	87.5	1.1237	0.9516
38.5	0.8590	0.8521	88.5	1.1257	0.9629
39.5	0.8661	0.8507	89.5	1.1274	0.9756
40.5	0.8732	0.8493	90.5	1.1284	0.9898
41.5	0.8802	0.8480	91.5	1.1292	1.0058
42.5	0.8872	0.8468	92.5	1.1294	1.0245
43.5	0.8941	0.8458	93.5	1.1285	1.0500
44.5	0.9009	0.8448	94.5	1.1268	1.0812
45.5	0.9078	0.8440	95.5	1.1240	1.1192
46.5	0.9145	0.8433	96.5	1.1190	1.1779
47.5	0.9212	0.8427	97.5	1.1107	1.2684
48.5	0.9278	0.8422	98.5	1.0944	1.4753
49.5	0.9344	0.8418	99.5	1.0011	12.0740

5 Parameterisation for RH-dependence

The following figure compares the full BOREAM model and the parameterisation for total SOA mass concentration (including water) as a function of relative humidity (RH) at 2 intermediate NO_x levels.

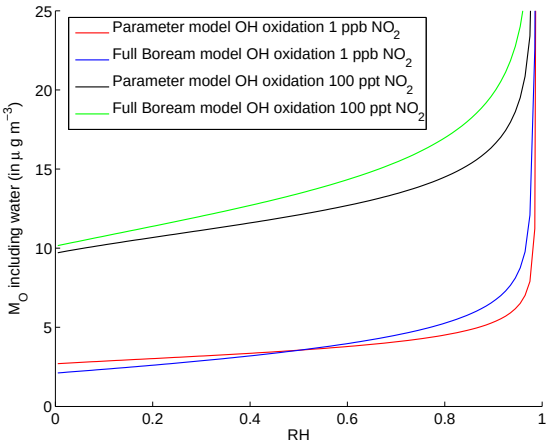

Figure 19: Parameterised and full model SOA mass loading M_O (including water) in function of RH, at 100 ppt and 1 ppb NO_2 for the OH-oxidation scenario (at 298 K).

References

Atkinson, R. et al.: Evaluated kinetic and photochemical data for atmospheric chemistry: Volume II - gas phase reactions of organic species, Atmos. Chem. Phys., 6, 3625–4055, 2006.

Capouet, M. and Müller, J.-F.: A group contribution method for estimating the vapour pressures of α-pinene oxidation products, Atmos. Chem. Phys., 6, 1455–1467, 2006.

Capouet, M., Peeters, J., Nozière, B., and Müller, J.-F.: α-pinene oxidation by OH: simulations of laboratory experiments, Atmos. Chem. Phys., 4, 2285–2311, 2004.

Capouet, M., Müller, J.-F., Ceulemans, K., Compernolle, S., Vereecken, L., and Peeters, J.: Modeling aerosol formation in α-pinene photooxidation experiments, J. Geophys. Res., 113, D02 308, doi:10.1029/2007JD008995, 2008.

Carter, W. P. L.: Documentation of the SAPRC-99 chemical mechanism for VOC reactivity assessment, final report to California Resources Board, contracts 92-329 and 95-308, Tech. rep., Air Pollut. Res. Cent.for Environ. Res. and Technol., Univ. of California, Riverside, California, URL `http://.www.cert.ucr.edu/ carter/reactdat.htm`, 2000.

Ceulemans, K., Compernolle, S., Peeters, J., and Müller, J.-F.: Evaluation of a detailed model of secondary organic aerosol formation from alpha-pinene against dark ozonolysis experiments, Atmos. Environ., 40, 5434–5442, 2010.

Jenkin, M. E., Hurley, M. D., and Wallington, T. J.: Investigation of the radical product channel of the $CH_3C(O)O_2$ + HO_2 reaction in the gas phase, Phys. Chem. Chem. Phys., 9, 3149–3162, 2007.

Makar, P. A.: The estimation of organic gas vapour pressure, Atmos. Environ., 35, 961–974, 2001.

Neeb, P.: Structure-reactivity based estimation of the rate constants for hydroxyl radical reactions with hydrocarbons, J. Atmos. Chem., 35, 295–315, 2000.

Ng, N. L., Chhabra, P. S., Chan, A. W. H., Surratt, J. D., Kroll, J. H., Kwan, A. J., McCabe, D. C., Wennberg, P. O., Sorooshian, A., Murphy, S. M., Dalleska, N. F., Flagan, R. C., and Seinfeld, J. H.: Effect of NO_x level on secondary organic aerosol (SOA) formation from the photooxidation of terpenes, Atmos. Chem. Phys., 7, 5159–5174, 2007.

Paulson, S. E., Liu, D.-L., and Orzechowska, G. E.: Photolysis of heptanal, J. Org. Chem., 71, 6403–6408, 2006.

Saunders, S. M., Jenkin, M. E., Derwent, R. G., and Pilling, M. J.: Protocol for the development of the Master Chemical Mechanism, MCM v3 (Part A): tropospheric degradation of non-aromatic volatile organic compounds, Atmos. Chem. Phys., 3, 161–180, 2003.

Schurath, U. and Naumann, K.-H.: Chemical Mechanism Develoment (CMD), EUROTRAC-2 subproject, final report, Tech. rep., Int. Sci. Secr.t, GSF-Natl. Res. Cent. for Environ. and Health, Munich, Germany, 2003.

Valorso, R., Aumont, B., Camredon, M., Raventos-Duran, T., Mouchel-Vallon, C., Ng, N. L., Seinfeld, J. H., Lee-Taylor, J., and Madronich, S.: Explicit modelling of SOA formation from α-pinene photooxidation: sensitivity to vapour pressure estimation, Atmos. Chem. Phys. Discuss., 11, 10 121–10 158, 2011.

Vereecken, L. and Peeters, J.: Decomposition of substituted alkoxy radicals - part 1: a generalized structure-activity relationship for reaction barrier heights, Phys. Chem. Chem. Phys., 11, 9062–9074, 2009.